Design model and recommendations of column-foundation connection through socket with rough interfaces

Modelo e recomendações de projeto da ligação pilar-fundação por meio de cálice com interfaces rugosas

R. M. F. CANHA [a]
rejane_canha@yahoo.com.br

G. M. CAMPOS [b]
mazureki@sc.usp.br

M. K. EL DEBS [c]
mkdebs@sc.usp.br

Abstract

The present work proposes design models and recommendations for column-foundation connection through socket with rough interfaces, including the shear key configuration, the socket and the precast column base. In the experimental investigations, the behavior of socket and column as a monolithic connection was verified. However, for this to occur, the shear key dimensions must be between the limits suggested by the study. Considering the total transfer of internal forces in the connections, the vertical reinforcement should be designed based on the bending theory. The proposed model for the design of the transverse horizontal reinforcement, considering monolithic behavior of the connection, was found to be in good agreement with the observed experimental results. With adjustments to this model for the socket, a new model for the design of precast column bases is proposed and compared with other model adapted for rough interfaces.

Keywords: socket foundation, precast columns base, rough interfaces, shear keys, pedestal walls

Resumo

Nesse trabalho, são propostos modelos e recomendações de projeto para a ligação pilar-fundação por meio de cálice com interfaces rugosas, incluindo a configuração das chaves de cisalhamento, o cálice e a base do pilar pré-moldado. Nas investigações experimentais abrangidas neste estudo, foi constatado que nas ligações rugosas ocorre o funcionamento conjunto do cálice com o pilar como em uma ligação monolítica. Entretanto, para que isso ocorra, é necessário que as dimensões das chaves de cisalhamento estejam entre os limites recomendados nesse estudo. Considerando a transferência total de esforços na ligação, a armadura vertical deve ser dimensionada segundo a teoria de flexão. O modelo proposto para o dimensionamento da armadura horizontal transversal, também baseado no comportamento monolítico da ligação, forneceu bons resultados quando comparados com os valores experimentais. A partir desse modelo calibrado para o cálice, é proposta uma nova formulação para a base do pilar pré-moldado, a qual é comparada com outro modelo adaptado para interfaces rugosas.

Palavras-chave: cálice de fundação, base de pilares pré-moldados, interfaces rugosas, chaves de cisalhamento, colarinho

[a]   Departamento de Engenharia Civil, Centro de Ciências Exatas e Tecnologia – Universidade Federal de Sergipe, rejane_canha@yahoo.com.br, Av. Marechal Rondon, s/n, Jardim Rosa Elze, CEP: 49100-000, São Cristóvão - SE, Brasil;
[b]   Departamento de Engenharia de Estruturas, Escola de Engenharia de São Carlos – Universidade de São Paulo, mazureki@sc.usp.br, Av. Trabalhador SãoCarlense, 400, CEP: 13566-590, São Carlos - SP, Brasil;
[c]   Departamento de Engenharia de Estruturas, Escola de Engenharia de São Carlos – Universidade de São Paulo, mkdebs@sc.usp.br, Av. Trabalhador SãoCarlense, 400, CEP: 13566-590, São Carlos - SP, Brasil.

1. Introduction

The column-foundation connection through socket consists of embedding part of the precast column into the cavity of the foundation element. This connection is widely used in precast concrete structures all over the world, being the most widespread in Brazil compared to other available types of column-foundation connections. This work presents a complementary analysis of the socket foundation initiated in Canha & El Debs [1], in which a critical analysis of available models and recommendations for socket are presented, and in Canha & El Debs [2], which proposes a design model for this element. These two abovementioned publications, however, are focused mainly on friction models for smooth socket foundation. More recently, Campos et al. [3] presented indications for the structural analysis of the column base in smooth interface sockets. The present work aims at presenting a complete structural analysis and detailing approach to precast column-socket connections with rough interfaces, including a configuration of this type of interface with shear keys proposed by Canha [4], refined design models proposed by Campos [5] and recommendations for rough socket foundation of the latter author. Based on Campos [5], it is easy to

confirm that some questions relative to column-socket connection with rough interfaces, such as the column base, still remain unsolved. On the other hand, Canha [4] indicated that smooth socket model can be applied to the case of rough interfaces by simply adjusting the friction coefficient to 1.0. This approach was adopted in the present work by adapting the model proposed by Campos et al. [3] to the rough column base. To complement the formulations and recommendations proposed, a new model is proposed for analysis and detailing the rough column base based on the monolithic behavior of rough connections pointed out by Canha [4]. The results of two analysis models for column bases are then confronted.

2. Model and recommendations for the design of rough socket

2.1 Rough interface configuration

A socket foundation connection is defined as rough when shear keys, responsible by the load transfer between the column and socket, are executed in the internal socket walls and on the precast column along the embedment region. Besides the contribution of bond and friction,

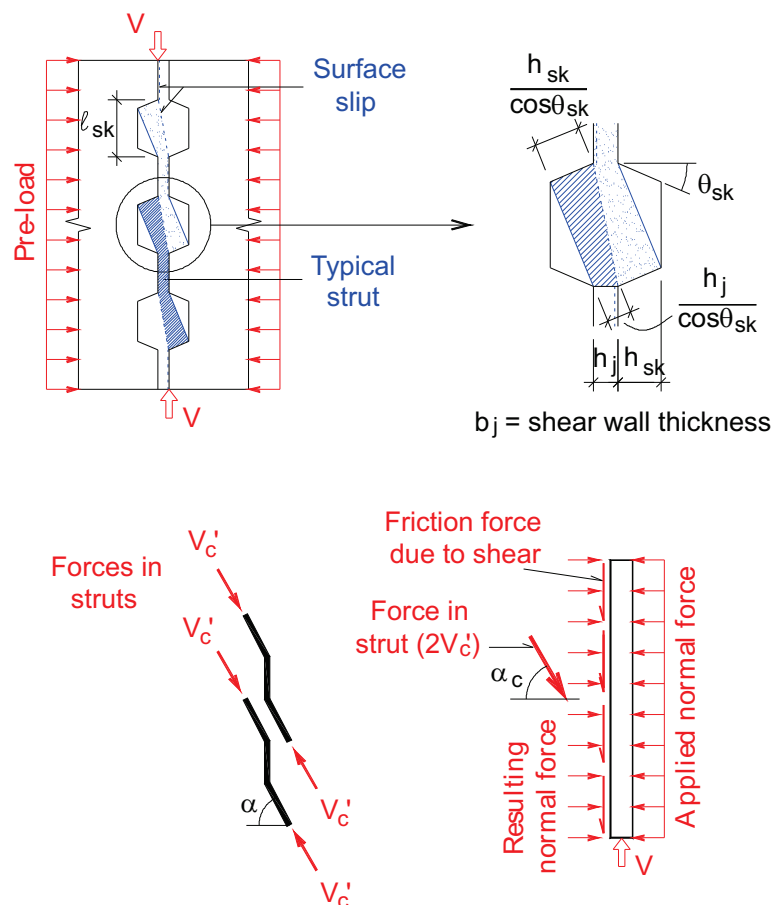**Figure 1 – Model for determining the maximum shear strength (Rizkalla et al. (7))**
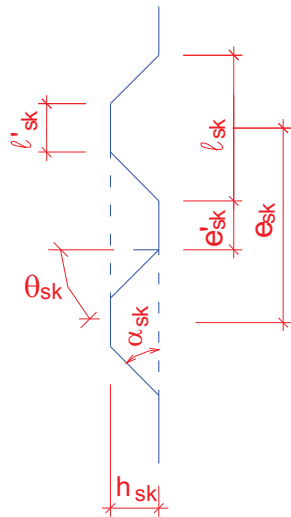
Figure 2 – Shear key variables (Canha (4))

these keys provide an additional portion of the interface shear strength on account of interlock mechanical fraction of the adherence. Nonetheless, besides those provided by NBR 9062:2006 [6], there are still no known specific recommendations for the analysis of these keys which guarantee an appropriate transfer of load in rough connections. In order to substantiate the adopted shear key dimensions of the rough column-socket connection tested by Canha [4], the theoretical model illustrated in Figure 1 proposed by Rizkalla et al [7] was used for the qualitative and systematic analysis of the geometric parameters of the shear keys. This model is commonly used for shear strength analysis of shear walls with shear keys and fixed together by dry mortar ("drypack"). The model was then adjusted with experimental tests carried out on specimens with smooth interface and with two shear key configurations labeled small and large shear keys. Based on the observed post-cracking behavior of the specimens, the maximum shear load (V) of the connections with shear keys can be estimated according to equation 1. In this equation, the first term represents the compressive strength of the concrete strut between diagonal cracks (V_c) while the second term refers to the strength due to friction along the sliding surface (V_f). The shear key geometrical parameters are given in Figure 2.

$$V = (n_{sk} - 1)f_{cr}A_{cs}\, \mathrm{sen}\,\alpha_c + \mu(\sigma_n A_c - (n_{sk} - 1)f_{cr}A_{cs}\cos\alpha_c) \quad (1)$$

Where:

n_{sk} is the number of shear keys

f_{cr} is the compressive strength of the cracked joint

$A_{cs} = \frac{1}{2}(h_j + h_{ch})b_j / \cos\theta_{ch}$ is the average transverse section of the diagonal section of the concrete strut

$\alpha_c = \tan^{-1}(\ell_{ch} / h_j)$ is the inclination of the diagonal section of the concrete strut relative to the horizontal.

The Figure 2 presents the following parameters:

e_{sk}: Distance between the shear key axes

e'_{sk}: Internal distance between shear keys

h_{sk}: Shear key height

ℓ_{sk}: Largest shear key base dimension

ℓ'_{sk}: Smallest shear key base dimension

α_{sk}: Inclination of shear key face relative to a parallel line through the joint axis

λ_{sk}: Ratio of largest base dimension to height of shear key

θ_{sk}: Inclination of shear key face relative to a perpendicular line through the joint axis.

The geometrical ratio of the shear key can be defined according to equation 2:

$$\lambda_{sk} = l_{sk} / h_{sk} \quad (2)$$

The main results obtained on applying the model proposed by Rizkalla et al. [7] are presented in Figure 3.

Figure 3(a) shows an increase in shear strength as the face angle of shear key α_{sk} decreases up to the limiting value of $\alpha_{sk, lim}$ for which the smallest shear key base dimension ℓ_{sk}' is null. This value of $\alpha_{sk, lim}$ was found to be 45° and 35° for small and large shear keys, respectively. It is worth pointing out that, according to Lacombe and Pommeret [8], when this angle is less than 45°, the failure of the connection takes place by slipping between the shear keys.

By increasing ℓ_{sk} and keeping the shear key height h_{sk} and the angle α_{sk} fixed, the value of λ_{sk} increases, thus resulting in an decrease in shear strength as illustrated by Figure 3(b). Still relative to λ_{sk}, it is noticed that the strength decrease is more pronounced along the first part of the curve up to the limiting value of λ_{sk}=6 indicated by Lacombe and Pommeret [8], and from this point, the strength is small and then tends to a constant value for large values of λ_{sk}. According to Figure 3(c), the increase in λ_{sk} as h_{sk} decreases is also one of the reasons for the observed decrease in shear strength V.

By varying the number of shear keys n_{sk}, the distance between keys e_{sk} is observed to decrease as the number of shear keys increases, consequently resulting in an increase in shear strength V, as illustrated by Figure 3(d).

Based on the theoretical study of the Rizkalla et al. [7] model, it is expected that a geometrical ratio of the key $\lambda_{sk} \leq 6$ provides appropriate stress transfer at the column-pedestal wall interface. Adopting shear keys with angle $\alpha_{sk} = 45°$, internal spacing $e'_{sk} = 4cm$ and the maximum ratio $\lambda_{sk} = 6$ to account for shear key symmetry on the reverse side of the interface, a suitable shear stress transfer occurs between the column and the socket.

The Brazilian Standard Code NBR 9062:2006 [6] recommends a minimum roughness of $h_{sk} = 1cm$ for every 10 cm of joint in order to assure a monolithic behavior of the connection. However, it does not specify what distance this 10 cm of joint refers to. Hence, the 10 cm will be considered here to represent the sum of the largest shear key base dimension ℓ_{sk} and the internal spacing between the shear keys e'_{sk}, thus resulting to a single key for each joint length considered, as illustrated in Figure 4(a).

For minimum shear key dimensions, it is recommended that the

largest shear key base dimension be twice the maximum size of the coarse aggregate and the shear key height be at least half the aggregate size, as illustrate in Figure 4(b), to guarantee that the coarse aggregate fits into the shear key during the concrete placement. In the case of symmetrical keys, it is necessary to consider the maximum size of the coarse aggregate relative to the largest of the three "concretes" of the connection (socket, column and joint).

To define the roughness to be adopted in the specimens tested by Canha [4], the shear keys were manufactured according to the limits imposed by NBR 9062:2006 [6] and the results presented regarding the parametric evaluation with the Rizkalla et al. [7] model. Two shear key configurations were used, one with maximum dimensions shown in Figure

4(a) referring to specimen IR1, and the other with dimensions a little less than the minimum values indicated in Figure 4(b) for specimen IR2.

Detailed experimental-theoretical studies of the socket foundation carried out by Canha [4] showed that the behavior of specimens with rough interfaces is similar to that of monolithic connections. The observed experimental strengths for the two tested specimens were verified to agree closely. Besides, the specimen with small shear keys (IR2) was found to present a higher stiffness (relative to rebar strains) than the specimen with large shear keys (IR1), as shown in Figure 5. The abovementioned observation indicates that the modification of shear key dimensions within the ranges indicated in Figure 4 does not influence, except the connection stiffness, the connection strength.

Figure 3 – Parametric evaluation of the shear keys using the model proposed by RIZKALLA et al. (7)
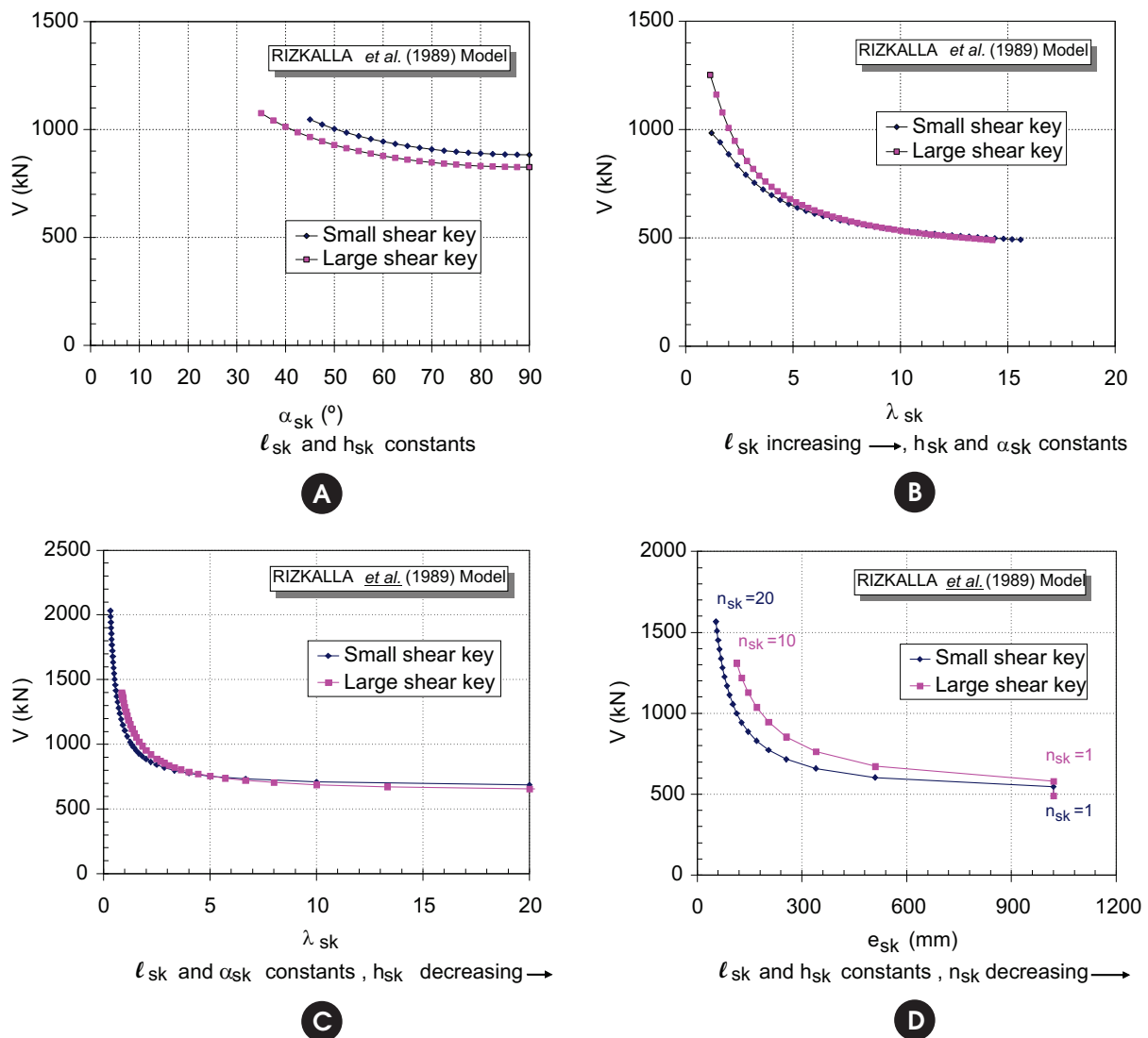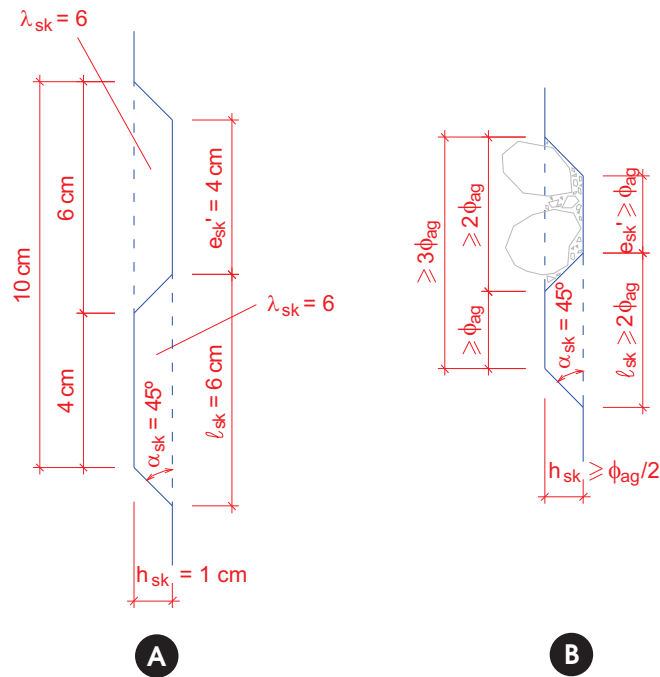
Figure 4 – (a) Maximum shear key dimensions with respect to minimum roughness according to NBR 9062:2006 (6) and theoretical evaluation according to Canha (4); (b) Minimum shear key dimensions as a function of aggregate dimension recommended by Canha (4)


2.2 Main vertical reinforcement – $A_{s,mv}$

The main vertical reinforcement $A_{s,mv}$ is defined as that distributed along the corners of the longitudinal and transverse walls. This

reinforcement, shown in Figure 6, has strength function on the tension side of the connection, but is placed symmetrically at the corners due to construction aspects.

Based on observation by Canha [4] that rough interface specimens

Figure 5 – Applied load-main vertical reinforcement strain curve (Canha (4))
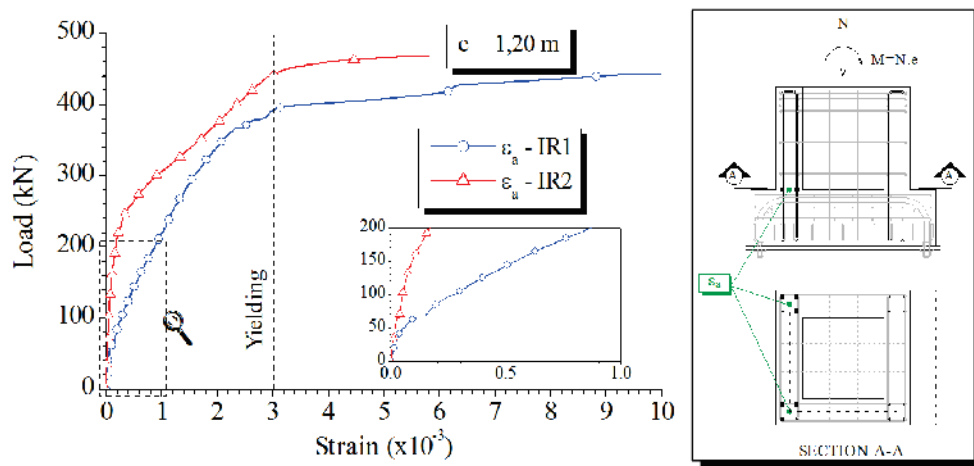
showed a similar behavior to that of monolithic connections, hence resulting in full transfer of the bending moments and normal loads from column to socket, it is recommended, for the case of rough interface sockets, to apply the bending theory for designing the main vertical reinforcement. Nonetheless, tests carried out by Jaguaribe Jr. [9] showed that the estimated connection strength based on the bending theory for reduced embedded lengths was higher than experimental strength values obtained from tested specimens. This indicated that the bending theory is applicable only to sockets with embedded lengths that meet the criteria given by the Brazilian Standard Code NBR 9062:2006 [6].

In this paper, a refined model for detailing the vertical reinforcements is presented, originally proposed by Canha [4], with additional considerations and recommendations, as shown in Figure 7. For a more precise analysis, it is recommended take into account all vertical reinforcements contributing to the strength of the connection. Besides this, the rectangular-parabolic concrete compression stress diagram should be adopted.

However, for practical applications, a simplified analysis can be employed. This approach assumes a simplified diagram of concrete compression stress with height equal to 0.8 of the depth of the neutral axis and the resulting tensile force determined by the contribution of the main vertical reinforcements at the corners of rear wall and the secondary vertical reinforcements placed in this wall. Hence, the estimated total reinforcement based on the bending theory is obtained from equation 3 and the reinforcement $A_{s,mv}$ is then calculated.

$$A_{s,tot} = 2 \cdot A_{s,mv} + A_{s,tsv} \qquad (3)$$

The secondary reinforcements of rough interface sockets are designed considering the behavior of the longitudinal walls similar to that of short corbel. It is noted that, in the application of bending theory, the reinforcement $A_{s,tsv}$ is included in the calculation of $A_{s,tot}$ and it is equal to $0.40 \cdot A_{s,mv}$. This secondary reinforcement is important in socket foundation to resist secondary stresses and for crack control of the pedestal walls.

Figure 7 shows the following parameters:

M_{bd}: Design bending moment at socket base

R_{csf}: Resultant of concrete compressive stress of socket

$R_{ssf} = R_{ssf1}$: Resultant of forces in vertical reinforcements $2 \cdot A_{s,mv} + A_{s,tsv}$ at $d_1 = d_{sf}$

R_{ssfi}: Resultant of forces in secondary vertical reinforcements $A_{s,lsv}$ at d_i. In the case of secondary vertical reinforcement in two layers, for instance, there are the following parameters:

R_{ssf2}: Resultant of forces in secondary vertical reinforcements $A_{s,lsv}$ at d_2

R_{ssf3}: Resultant of forces in secondary vertical reinforcements $A_{s,lsv}$ at d_3

σ_{cd}: Design concrete compressive stress of socket

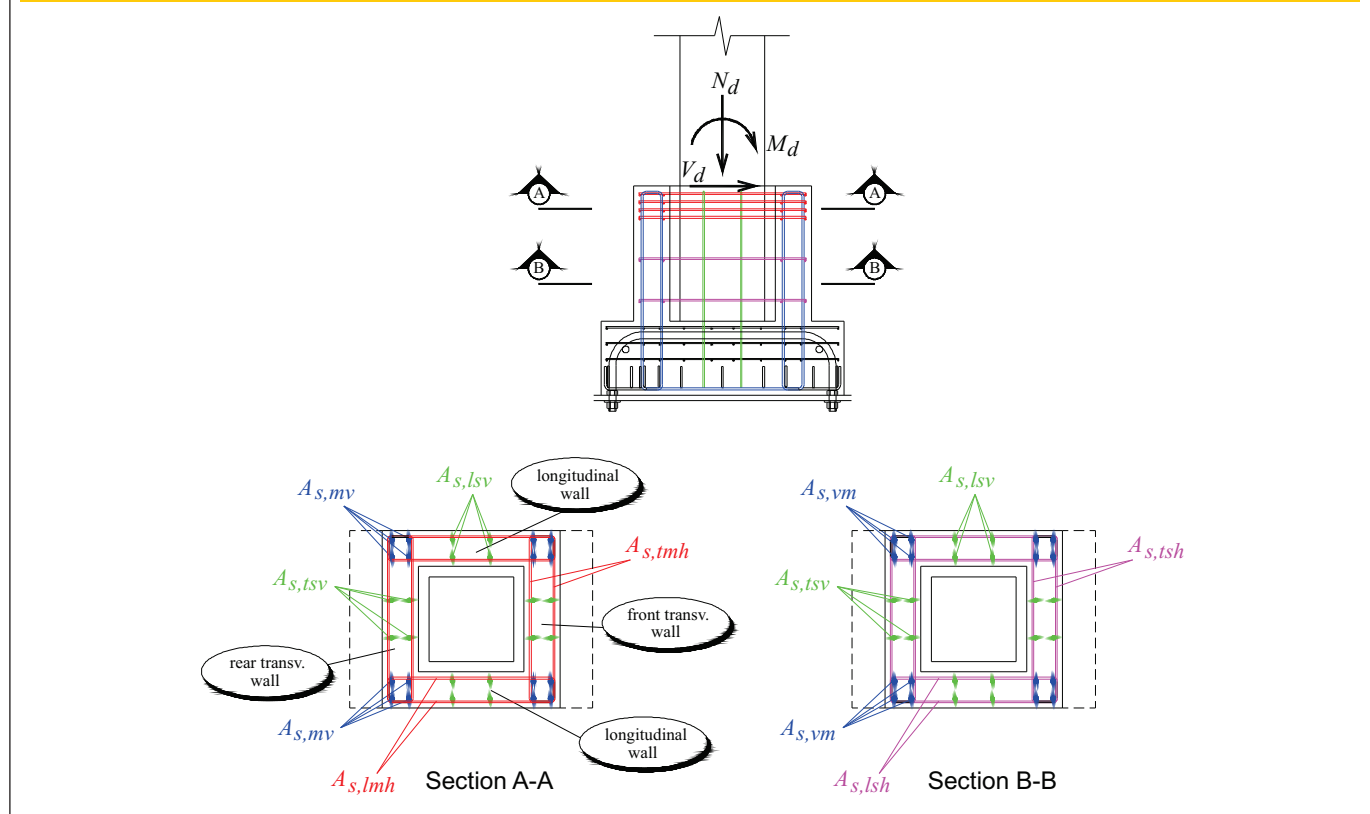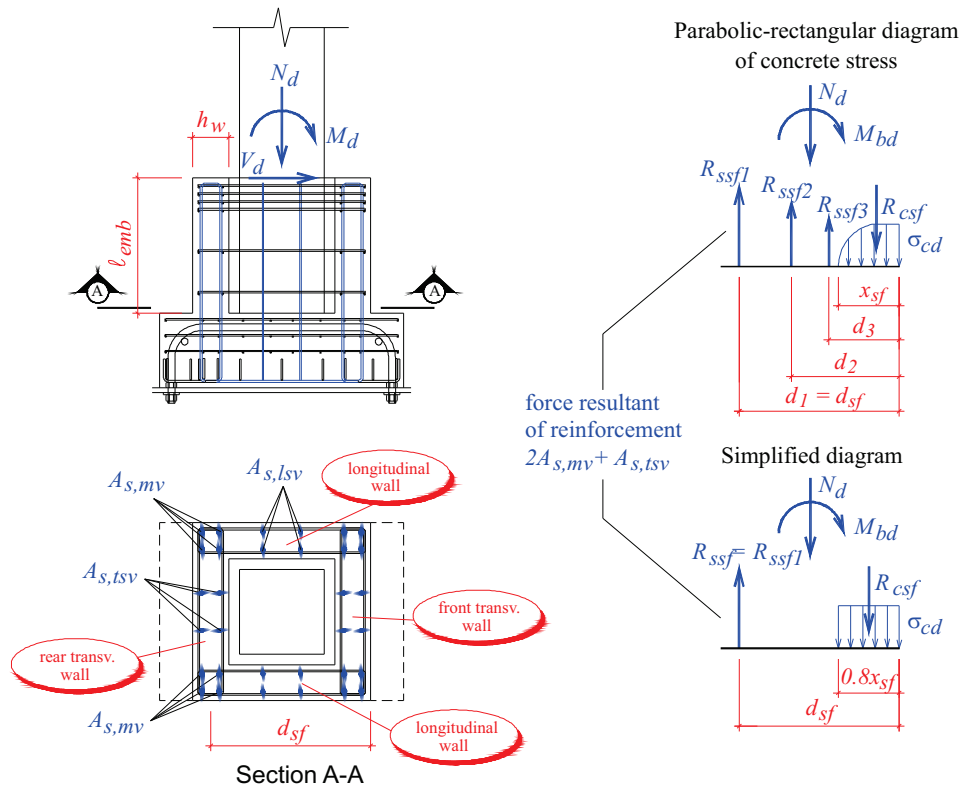## Figure 6 – Positioning of pedestal reinforcements

Figure 7 – Schematic representation of force for the determination of vertical reinforcements in rough interface sockets according to Canha (4)

X_{sf}: Depth of neutral axis

For a simplified bending theory analysis, the force R_{ssf}, resultant in the vertical reinforcements $2.A_{s,mv} + A_{s,tsv}$, is determined according to the equation:

$$R_{ssf} = A_{s,tot} \cdot f_{yd} = \frac{M_{bd} - N_d \cdot (z_{sf} + 0.5 \cdot h_w - 0.5 \cdot h_{ext})}{z_{sf}} \quad (4)$$

Where:

$M_{bd} = M_d + V_d \cdot l_{emb}$

$z_{sf} = d_{sf} - 0.4 \cdot x_{sf}$

For practical application in the case of large eccentric normal forces, the parameters $z_{sf} \cong 0.9 \cdot d_{sf}$ and $d_{sf} \cong 0.9 \cdot h_{ext}$ could be used. The resultant of concrete compression stresses in the socket is estimated as:

$$R_{csf} = R_{ssf} + N_d = \frac{M_{bd} + N_d \cdot (0.5 \cdot h_{ext} - 0.5 \cdot h_w)}{z_{sf}} \quad (5)$$

Substituting $z_{sf} = d_{sf} - 0.4 \cdot x_{sf}$ in equations 3 and 4, the resultants

R_{ssf} and R_{csf} are calculated according to expressions 6 and 7, respectively, as:

$$R_{ssf} = \frac{M_{bd} - N_d \cdot (0.5 \cdot h_{ext} - 0.4 \cdot x_{sf})}{d_{sf} - 0.4 \cdot x_{sf}} \quad (6)$$

$$R_{csf} = \frac{M_{bd} + N_d \cdot (0.5 \cdot h_{ext} - 0.5 \cdot h_w)}{d_{sf} - 0.4 \cdot x_{sf}} \quad (7)$$

Considering that the force R_{csf} is the resultant of the compressive stresses σ_{cd} considered uniformly distributed on an area of $0.8 \cdot x_{sf} \cdot h_{ext}$, for the rectangular compressive stress diagram, the force R_{csf} results in:

$$R_{csf} = A_{csf} \cdot \sigma_{cd} = 0.8 \cdot x_{sf} \cdot h_{ext} \cdot \sigma_{cd} \quad (8)$$

Substituting equations 6 and 8 in equation 5, the position of the neutral axis can be determined from equation 9, and subsequently $A_{s,mv}$ is determined.

$$M_{bd} - 0.5 \cdot N_d \cdot h_{ext} + N_d \cdot d_{sf} - 0.8 \cdot x_{sf} \cdot h_{ext} \cdot \sigma_{cd} \cdot d_{sf} + 0.32 \cdot x_{sf}^2 \cdot h_{ext} \cdot \sigma_{cd} = 0 \quad \text{(9)}$$

If the simplified rectangular concrete compressive stress diagram is adopted, it results, for the socket, a constant compressive stress of $\sigma_{cd} = 0.85 \cdot f_{cd}$ along a depth of $0.8 \cdot x_{sf}$ measured from the compression face, referred to compressed zone of constant height. For the remaining height of $0.2 \cdot x_{sf}$, the compressive stresses in concrete is neglected.

2.3 Main horizontal reinforcements

The main horizontal reinforcement consists of the main transverse horizontal reinforcement, $A_{s,tmh}$ and the main longitudinal horizontal reinforcement, $A_{s,lmh}$. $A_{s,tmh}$ is the reinforcement distributed along the top of the transverse walls within a distance of $\ell_{emb}/3$ from the top while $A_{s,lmh}$ is that distributed along the top of the longitudinal walls within $\ell_{emb}/3$. Since the reinforcements $A_{s,lmh}$ and $A_{s,tmh}$ are distributed within the same height of the rough socket, and considering the positioning of the rebars in the socket at the construction, it is recommended, when designing socket connections, to adopt the largest reinforcement area with the reinforcement arranged symmetrically. Figure 6 shows the positioning of these reinforcements.

2.3.1 Main transverse horizontal reinforcement – $A_{s,tmh}$

Canha et al. [10] proposes a model for the analysis of transverse walls of sockets with smooth and rough interfaces, based on the experimental results of Canha [4] and Jaguaribe Jr. [9]. Following the experimental results of Nunes [11] obtained from the behavior of the transverse walls, a refined Canha et al. [10] model presented herein was obtained. Figure 8 presents the stress transfer model from column to socket with rough interfaces, based on Canha et al. [10].

In this model, compression struts appear on the compressed side (front transverse wall) due to the transfer of the compression resultant R_c from the column to the front wall, thus resulting in a force R_{csf} in the socket foundation. Due to the presence of these compression struts, a pressure resultant H_f is observed to act on the front transverse wall. This pressure attains its maximum value at the top of the front transverse wall due to the smaller inclinations of the struts with respect to a horizontal axis through the top of this wall. Since these struts are practically vertical near the socket base, the pressure at this point is null. This force H_f can determined using equation 10 below:

$$H_f = \frac{R_{csf}}{\tan \beta_f} \quad \text{(10)}$$

Figure 8 – Transfer of forces resultants from column to rough socket (adapted from Canha et al. (10))

Transfer of forces resultants
from column to socket foundation

Rear transverse
wall

Front transverse
wall
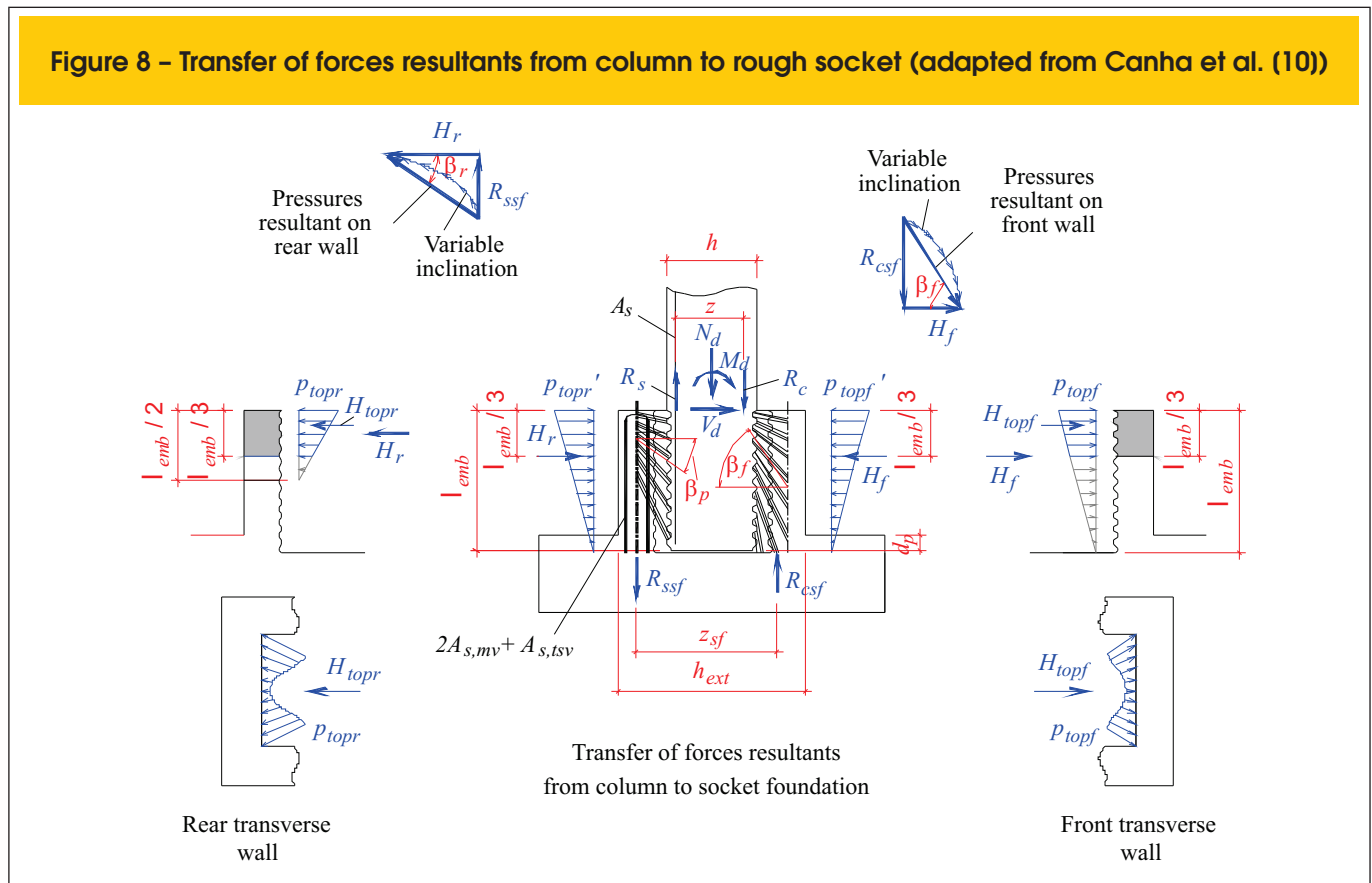
where:

β_f : average struts inclination on the compression side.

R_{csf} : Compression force resultant in the socket determined from equation 5.

On the compression side of the column, the pressures distribution is similar to that of the front wall. Hence, the pressures at the top of the column and of the front wall are the same:

$$p_{topf}{}' = p_{topf} \qquad \text{(11)}$$

The pressure resultant H_{topf} is thus equal to the resultant of the trapezoidal pressure block acting at the top of the front transverse wall. This means that H_{topf} is a portion of H_f and is determined according to equation 12:

$$H_{topf} \cong 0{,}6 \cdot H_f \qquad \text{(12)}$$

On the tension side (rear transverse wall), the transfer by compression struts of most of the tension force R_s , from the column to the rear wall, results in the tension force R_{ssf} in the socket and in the

pressure H_r on the rear wall. It can be noticed that the pressure H_r is concentrated mostly at the top of the wall due to the smaller inclination of the compression struts in this region relative to the horizontal axis, and the base of the rear transverse wall does not transmit forces. The pressure H_r is determined by equation 13 as:

$$H_r = \frac{R_{ssf}}{\tan \beta_r} \qquad \text{(13)}$$

where:

β_r : average compression struts inclination on the tension side.

R_{ssf} : Force resultant in the vertical reinforcements $2.A_{s,mv} + A_{s,tsv}$ calculated by equation 4.

In case of the tensile side of the column, the compression struts are known to initiate at the bottom of the column. Because of this, the triangular pressure distribution occurs all over the tensioned column base with length ℓ_{emb}, such that the pressure at the column top is half of that acting on the rear wall:

$$p_{topr}{}' = \frac{p_{topr}}{2} \qquad \text{(14)}$$

Figure 9 – Design model proposed for the front and rear walls of socket with rough interfaces (Canha et al. (10)))

Plan of front transverse wall

Plan of rear transverse wall
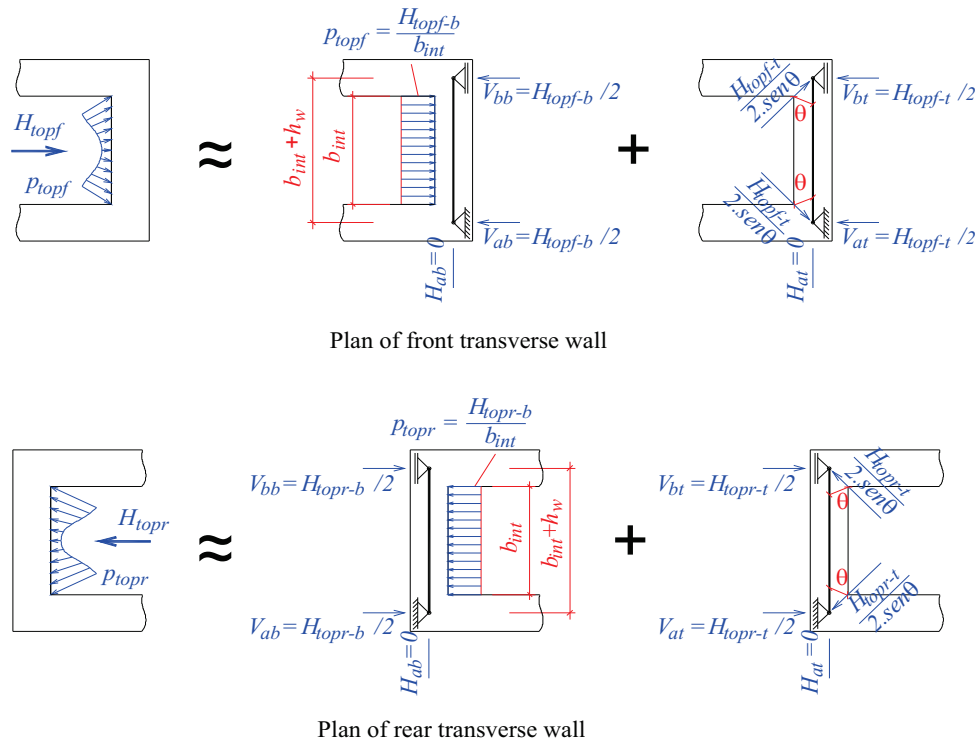
The pressure resultant H_{topr} on the upper third of the rear transverse wall is approximately equal to the pressure H_r distributed on the upper half of that wall.

Experimental results confirmed that the upper part of the front and rear transverse walls of rough sockets were subjected to combined bending and tension, with the predominance of tension. This behavior under bending-tension was observed from obtained reinforcement strains and cracks configuration of the transverse walls. Hence, the proposed analysis model presented in Figure 9, based on the experimental investigation, consists of representing the top of transverse walls as a simply supported beam with the distributed pressure given by two parts: a pressure H_{topf-b} and H_{topr-b} which causes bending of the beam, and a pressure H_{topf-t} and H_{topr-t} that is transmitted to the beam supports at an angle of θ=45º, representing the average crack inclination of the tested specimens, causing tension of the beam. The total upper pressure on the front wall H_{topf} and on the rear wall H_{topr} is the sum of the portions referring to bending and tension.

Based on the obtained strain gauge results, the percentages adopted for the case of bending- tension was 15% for pressures H_{topf-b} and H_{topr-b}, and 85% for pressures H_{topf-t} and H_{topr-t}. Besides these percentages, only the tension force, for which $H_{topf} = H_{topf-t}$ and $H_{topr} = H_{topr-t}$, can be considered.

Concerning the average inclination of the compression struts of the walls, Canha et al. [10] indicates a value of 45º for β_f and β_r. However, it is noticed that, in some cases, with these inclination angles, the theoretical results did not represent well the experimental results. Because of this, an analysis with the variation of the average inclinations of the compression struts in the front and rear transverse walls was developed. The obtained results were then complemented with experimental results of Nunes [11]. For the angle β_f, the values of 45º and 60º were compared, and for β_r, the values of 45º and 35º.

An analysis and comparative study of the experimental and theoretical results was carried out for specimens IR-1 and IR-2 tested by Canha [4], for IR-3 by Jaguaribe Jr. [9] and for IR-4 by Nunes [11]. Table 1 presents the results of the force in the reinforcement $A_{s,tmh}$ with variation in β_f of the front transverse wall.

Analyzing the results, for all cases when $\beta_f = 60^o$ was considered, the obtained theoretical and experimental forces showed close agreement. For instance, for specimen IR-2, considering the bending-tension and an angle of 60º, the difference between the theoretical and experimental force was found to be approximately 132%, compared to approximately 300% when a strut inclination of 45º was taken into account.

However, considering the bending-tension, and $\beta_f = 60^o$ for specimen IR-3, the theoretical internal force was found to be below the observed experimental result. It is noteworthy however that this specimen

Table 1 – Theoretical and experimental internal forces in reinforcement A_{s,tmh} with varying angles of β_f for the front transverse wall of rough interface sockets

Specimen	Design model	Angle β_f	$R_{s,tmhe}$ (kN)		$R_{s,tmhi}$ (kN)	
			Theoretical	Experimental	Theoretical	Experimental
IR-1	Bending-tension	45°	205.5		41.8	
		60°	118.6	87.0	24.1	15.7
	Tension	45°	145.5		145.5	
		60°	84.0		84.0	
IR-2	Bending-tension	45°	206.8		42.1	
		60°	119.4	51.4	24.3	9.9
	Tension	45°	146.4		146.4	
		60°	84.5		84.5	
IR-3	Bending-tension	45°	172.4		33.6	
		60°	99.5	42.0	19.4	20.5
	Tension	45°	121.1		121.1	
		60°	69.9		69.9	
IR-4	Bending-tension	45°	208.2		25.2	
		60°	120.2	54.9	14.5	4.2
	Tension	45°	137.3		137.3	
		60°	79.3		79.3	

had been tested by Jaguaribe Jr. [9] with a reduced embedded length and consequently the observed deviation of the experimental results was due mainly to this factor. On the other hand, considering only tension and an angle of 60º for specimen IR-1, the obtained theoretical force in the external branch was found to be approximately 3.5% below the experimental result. In determining the experimental values, however, a modulus of elasticity of 210 GPa for the reinforcement steel was adopted even though it may be slightly lower, thus making up for this small difference.

A general analysis showed that the theoretical model which best represents the experimental results is that corresponding to an average strut inclination of 60º on the compression side of the socket foundation. Based on this, a strut angle of 60º will be adopted in the present study.

Although the observed percentage differences are large, it is important to highlight here that the two other models cited in the literature for analysis of the front transverse wall were found to result in much higher differences compared to experimental results. Table 2 compares the experimental results with those of the proposed model, Melo [12] and CNR 10025:1998 [13] models. The bending theory based model by Melo [12] considers the upper part of front transverse wall as a beam on two fixed supports and subjected to bending moments, with resulting plastic bending moments at the extremities. The tension model given in CNR 10025:1998 [13,] however, recommends the application of a strut and tie model to the upper part of front transverse wall considering only the existence of tensile stresses in this re-

Table 2 – Comparison between the proposed model and that given by Melo (12) and CNR 10025:1998 (13)					
Specimen	**Design model**	**$R_{s,tmhe}$ (kN)**		**$R_{s,tmhi}$ (kN)**	
		Theoretica l	Experimental	Theoretica l	Experimental
IR-1	Proposed $\beta_f = 60°$ — Bending-tension	118.6		24.1	
	Tension	84.0	87.0	84.0	15.7
	Melo (12)	542.7		542.7	
	CNR 10025:1998 (13)	686.9		686.9	
IR-2	Proposed $\beta_f = 60°$ — Bending-tension	119.4		24.3	
	Tension	84.5	51.4	84.5	9.9
	Melo (12)	546.3		546.3	
	CNR 10025:1998 (13)	691.4		691.4	
IR-3	Proposed $\beta_f = 60°$ — Bending-tension	99.5		19.4	
	Tension	69.9	42.0	69.9	20.5
	Melo (12)	558.1		558.1	
	CNR 10025:1998 (13)	717.0		717.0	
IR-4	Proposed $\beta_f = 60°$ — Bending-tension	120.2		14.5	
	Tension	79.3	54.9	79.3	4.2
	Melo (12)	497.2		497.2	
	CNR 10025:1998 (13)	668.9		668.9	

Table 3 – Theoretical and experimental internal forces in reinforcement $A_{s,tmh}$ with varying angles o β_r for the rear transverse wall of rough interface sockets

Specimen	Design model	Angle β_r	$R_{s,tmhe}$ (kN)		$R_{s,tmhi}$ (kN)	
			Theoretical	Experimental	Theoretical	Experimental
IR-3	Bending-tension	45°	159.90		31.20	
		35°	228.40	100.30	44.50	46.50
	Tension	45°	112.40		112.40	
		35°	160.50		160.50	
IR-4	Bending-tension	45°	199.60		24.10	
		35°	285.10	101.30	34.50	33.80
	Tension	45°	131.60		131.60	
		35°	188.00		188.00	

gion. Table 3 presents the resulting forces in the reinforcement $A_{s,tmh}$ according to the variation of β_r of the rear transverse wall.

An analysis of Table 3 indicates that the compression struts inclinations on the tension side of the socket (rear wall) are smaller than those of the compression struts on the compression side (front wall). Hence, for this wall, angles of 35° and 45° were adopted in this study. The rear transverse wall was instrumented only in specimens IR-3 and IR-4. Table 3 shows the data for these two sockets.

As it can be perceived, for the two specimens under bending-tension condition, and considering an angle of 45°, the obtained theoretical forces in the internal branch of the reinforcement were smaller than the observed experimental values, hence this strut angle is not recommended to consider. If an angle of 35° is considered, the verification of forces for specimen IR-4 is not neglected. The theoretical force in specimen IR-3 was found to be slightly smaller that the observed experimental value, but as it can be recalled, this specimen had a reduced embedded length.

Notwithstanding the few experimental results available, it is recommended that a value of $\beta_r = 35°$ be adopted, because considering this situation, the theoretical force is higher than the experimental value. A strut angle of 30° was not considered since the corresponding results for this situation would be very conservative relative to tension or more still, would not meet safety conditions for the case of bending-tension.

It is worth emphasizing that in the knowledge of the authors, this formulation is currently the only model available for analyzing the rear transverse wall.

2.3.2 Main longitudinal horizontal reinforcement – $A_{s,lmh}$

As indicated in Figure 6, the reinforcement $A_{s,lmh}$ located on the upper part of the longitudinal walls of the rough socket must be determined considering the effect of the pressures H_{topf} and H_{topr} acting on the transverse walls of the socket.

The main horizontal reinforcement is made up of two branches: external and internal branch, and must be distributed in the upper part of the socket within a height of $\ell_{emb}/3$.

After determining the pressures acting on the transverse walls, it is recommended to estimate the resulting steel area based on the pressure on the front and rear walls. An estimate of this reinforcement is carried out following equations 15 and 16, and the adopted $A_{s,lmh}$ is the highest of the obtained values.

$$A_{s,lmh} = \frac{H_{topf}}{2 \cdot f_{yd}} \tag{15}$$

$$A_{s,lmh} = \frac{H_{topr}}{2 \cdot f_{yd}} \tag{16}$$

2.4 Secondary reinforcements – $A_{s,sv}$ and $A_{s,sh}$

Figure 6 illustrates the positioning of the secondary vertical reinforcement $A_{s,sv}$ and the secondary horizontal reinforcement $A_{s,sh}$.

These secondary reinforcements are used in socket foundation to resist secondary stresses and for cracking control of pedestal walls. It is noteworthy that the secondary horizontal reinforcements used in the front wall play the important role of absorbing the pressures within two lower thirds of these wall ($2\ell_{emb}/3$).

For calculation of the secondary reinforcements of socket with rough interfaces, it is recommended to apply the short corbel theory for the longitudinal walls, respecting the following areas and spacings indicated in El Debs [14]:

■ For secondary vertical reinforcement:
   $A_{s,sv} = A_{s,tsv} = A_{s,lsv} \geq 0.40 \cdot A_{s,mv}$
■ For secondary horizontal reinforcement:
   $A_{s,sh} = A_{s,tsh} = A_{s,lsh} \geq 0.25 \cdot A_{s,mv}$

For both vertical and horizontal secondary reinforcements, a spacing s between 150 mm and 300 mm must be adopted.

3. Model and recommendations for the design of rough column bases

3.1 Proposed model based on monolithic behavior

Although the experimental investigation carried by Canha [4] was focused mainly on pedestal walls, the observed monolithic behavior of rough interface connections indicates that detailing of the column base obeys the same bending theory.

As mentioned previously, based on the experimental results obtained by Nunes [11], it was possible to refine the model describing the transfer of load from the column to socket originally proposed by Canha et al. [10].

With the model calibrated for socket foundations, the forces acting on the column can be obtained, resulting in the proposed model shown in Figure 10.

The rough column base is subjected to H_f and H_r on the sides referring to the front and rear transverse walls, respectively, resulting from the transfer through struts of the internal compression and tension forces to these walls as presented in item 2.3.1.

Besides the mobilization of the friction forces, the use of shear keys on the inner pedestal walls and column faces permits the transfer of shear through interlock mechanical mechanism between shear keys. The proposed model considers the shear stresses on both the transverse and longitudinal walls as uniformly distribution. The shear stress resulting from the action of the bending moment (τ_M) is considered to act in the upward direction on the compression side and downward on the tension side. Meanwhile, the shear stress mobilized due to the normal force (τ_N) has an upward direction in all walls.

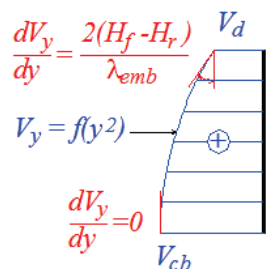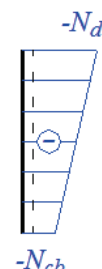Figure 10 – Design model proposed for the rough column base
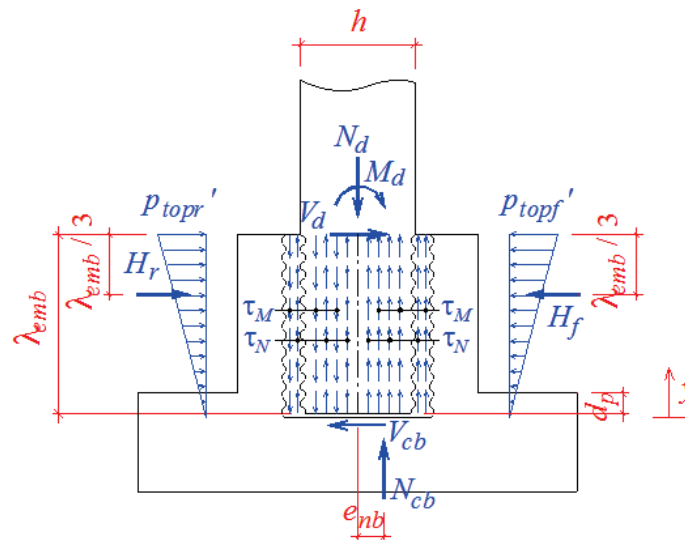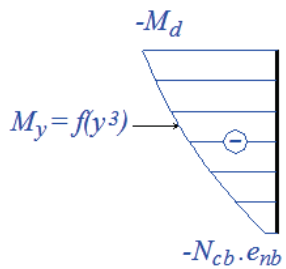
Also, at the column bottom, there is the internal transverse force V_{cb} and the internal eccentric normal force N_{cb}.
The problem thus involves four unknowns (τ_M, τ_N, V_{cb} and N_{cb}). Besides the three static equilibrium equations, there is an additional equation related to the normal reaction N_{cb} at the column bottom. This force is considered as the N_d reduced by ratio of the column cross section A_c to the external surface area of the pedestal A_{cp}, according to the following equation:

$$N_{cb} = N_d \frac{A_c}{A_{cp}} \quad (17)$$

Based on the structural outline of this element, the diagrams of the internal forces were determined with the corresponding expressions given below.
Considering a pressures variation along the embedded length ℓ_{emb}, for practical applications, the column transverse reinforcement area is determined for maximum internal forces.
Hence the $p_{topf}{}'$ and $p_{topr}{}'$ values are given, respectively, by equations 18 and 19:

$$p_{topf}' = \frac{2 \cdot H_f}{\ell_{emb}} = \frac{2 \cdot R_{csf}}{\ell_{emb} \cdot \tan\beta_f} \quad (18)$$

$$p_{topr}' = \frac{2 \cdot H_r}{\ell_{emb}} = \frac{2 \cdot R_{ssf}}{\ell_{emb} \cdot \tan\beta_r} \quad (19)$$

The shear force V_{cb} at the column bottom and the shear stress τ_N are determined from the equilibrium equations of forces in the horizontal and vertical directions and are given, respectively, by:

$$V_{cb} = V_d + H_r - H_f \quad (20)$$

$$\tau_N = \frac{N_d - N_{cb}}{(2h + 2b) \cdot \ell_{emb}} \quad (21)$$

From the moment equilibrium relative to point O, the shear stress τ_M can be defined by equation 22:

$$\tau_M = \frac{\dfrac{M_d}{\ell_{emb}} + V_d + \dfrac{2}{3}(H_r - H_f) - \dfrac{N_{cb} \cdot e_{nb}}{\ell_{emb}}}{h \cdot b + \dfrac{h^2}{2}} \quad (22)$$

The internal forces along the column base are calculated from the three static equilibrium equations in plane.
The bending moment M_y acting at a given distance y from the column bottom is calculated by the following equation:

$$M_y = -N_{cb} \cdot e_{nb} + \left(\frac{N_{cb} \cdot e_{nb} - M_d}{\ell_{emb}} + \frac{H_r - H_f}{3}\right) \cdot y - \frac{(H_r - H_f)}{3\ell_{emb}{}^2} y^3 \quad (23)$$

Also, the shear force V_y at a given distance y from the column bottom is given by:

$$V_y = V_d + H_r - H_f - \frac{(H_r - H_f)}{\ell_{emb}{}^2} y^2 \quad (24)$$

The internal normal force N_y at a given distance y from the column bottom is:

$$N_y = -N_{cb} + \left(\frac{N_{cb} - N_d}{\ell_{emb}}\right) \cdot y \quad (25)$$

The Bending Moment Diagram has a cubic shape. The absolute maximum value M_{max} at the column top and absolute minimum value M_{min} at the column bottom are given, respectively, by:

$$M_{max} = -M_d \quad (26)$$

$$M_{min} = -N_{cb} \cdot e_{nb} \quad (27)$$

On the other hand, a parabolic diagram is adopted for the Shear Force Diagram with the maximum value V_{max} at the column bottom and the minimum value V_{min} at the column top are calculated, respectively, by:

$$V_{max} = V_d + H_r - H_f \quad (28)$$

$$V_{min} = V_d \quad (29)$$

And lastly, the Axial Force Diagram has a trapezoidal shape with its maximum N_{max} value at the column top and the minimum

value N_{min} at the column bottom, given, respectively, by:

$$N_{max} = -N_d \tag{30}$$

$$N_{min} = -N_d \frac{A_c}{A_{cp}} \tag{31}$$

To determine the column longitudinal reinforcement, the largest values of the bending moment and the normal force acting at the section of column top are considered. For the transverse reinforcement, the column bottom section, where the maximum shear force is found to act, must be used. The determination of this reinforcement must consider shear concrete strength.

Besides determining the column reinforcements, whichever analysis model is employed, it is recommended that the column longitudinal reinforcement be properly anchored to the column base, and the vertical reinforcement of rear transverse wall be detailed by over lapping the reinforcement, in order to transfer the tensile force of column in proper form to the rear wall. Experimental results obtained from specimens tested by Canha [4] and Jaguaribe Jr. [9] confirm that for adequate transfer of force from the column to the socket, the minimum embedded length for column-socket foundation elements with rough interfaces must meet the NBR-9062:2006 [6] requirements.

As for smooth interfaces, the determination of the anchored length of the column longitudinal reinforcement is given by equation 32 based on recommendations by Leonhardt and Mönnig [15]. The stress transferred from reinforcement to concrete from this point of anchorage was confirmed experimentally for smooth specimens by Ebeling [16] and extrapolated here for rough specimens.
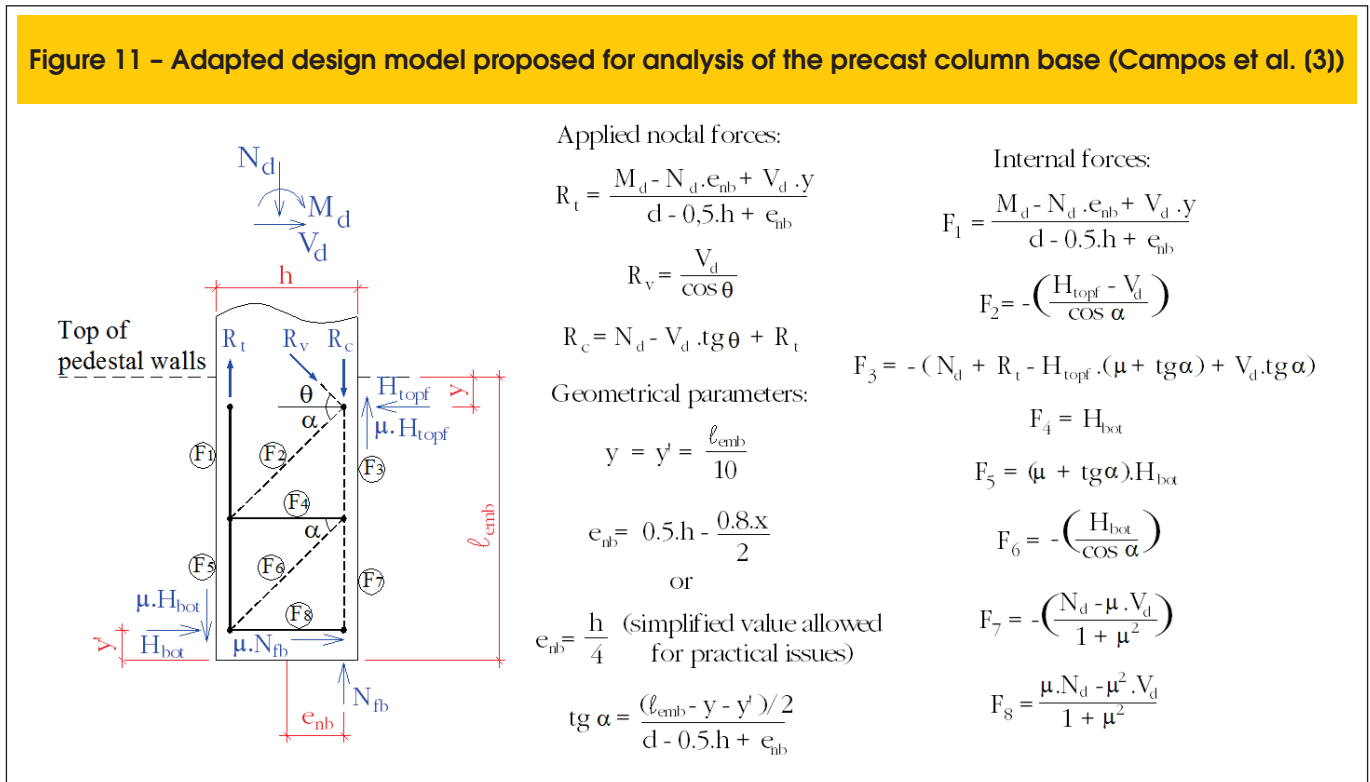
$$\ell_{anc} = \frac{\ell_{emb}}{2} \tag{32}$$

3.2 Adaptation of model considering friction forces

Campos et al. [3] proposes a strut-and-tie model applicable to the analysis of smooth precast column base, which was based on experimental results of Ebeling [16]. This model was adjusted with that proposed by Canha [4] for the design of smooth interface sockets considering the strength of concrete in the determination of internal forces and subsequently in calculating the transverse reinforcement. The adjusted model with the proposed modifications is given in Figure 11. The pressure on the front transverse wall H_{topf}, the pressure on the rear transverse wall H_{bot}, and the normal reaction on the foundation base N_{fb}, defined by the equilibrium equations, are given, respectively, by equations 33, 34 and 35:

$$H_{topf} = \frac{\dfrac{M_d}{d-0.5h+e_{nb}}+N_d \cdot \left(\dfrac{\mu^2}{1+\mu^2}-\dfrac{e_{nb}}{d-0.5h+e_{nb}}\right)+V_d \cdot \left(\dfrac{\mu}{1+\mu^2}+\dfrac{y}{d-0.5h+e_{nb}}+2\cdot tg\alpha\right)}{\mu+2\cdot tg\alpha} \tag{33}$$

Applied nodal forces:

$$R_t = \frac{M_d - N_d \cdot e_{nb} + V_d \cdot y}{d - 0.5h + e_{nb}}$$

$$R_v = \frac{V_d}{\cos\theta}$$

$$R_c = N_d - V_d \cdot tg\theta + R_t$$

Geometrical parameters:

$$y = y' = \frac{\ell_{emb}}{10}$$

$$e_{nb} = 0.5h - \frac{0.8 \cdot x}{2}$$

or

$$e_{nb} = \frac{h}{4} \quad \text{(simplified value allowed for practical issues)}$$

$$tg\,\alpha = \frac{(\ell_{emb} - y - y')/2}{d - 0.5h + e_{nb}}$$

Internal forces:

$$F_1 = \frac{M_d - N_d \cdot e_{nb} + V_d \cdot y}{d - 0.5h + e_{nb}}$$

$$F_2 = -\left(\frac{H_{topf} - V_d}{\cos\alpha}\right)$$

$$F_3 = -(N_d + R_t - H_{topf} \cdot (\mu + tg\alpha) + V_d \cdot tg\,\alpha)$$

$$F_4 = H_{bot}$$

$$F_5 = (\mu + tg\alpha) \cdot H_{bot}$$

$$F_6 = -\left(\frac{H_{bot}}{\cos\alpha}\right)$$

$$F_7 = -\left(\frac{N_d - \mu \cdot V_d}{1 + \mu^2}\right)$$

$$F_8 = \frac{\mu \cdot N_d - \mu^2 \cdot V_d}{1 + \mu^2}$$

$$H_{bot} = H_{topf} - \frac{\mu \cdot N_d + V_d}{1 + \mu^2} \tag{34}$$

$$N_{fb} = \frac{N_d - \mu \cdot V_d}{1 + \mu^2} \tag{35}$$

This model is indicated for sockets subjected to normal forces with high eccentricity and with embedded lengths based on NBR 9062:2006 [6] recommendations.

Canha [4] confirms that the design of socket foundations considering friction forces wherein the friction coefficient μ is adjusted to 1 was in the safe side for rough interface specimens, in spite of its being more conservative than the bending theory. Thus, the model for smooth column base was applied to rough column base analysis, considering $\mu = 1$, as a base for comparison with model proposed for rough column based on monolithic behavior.

3.3 Analysis of column base

To investigate the proposed model for column base, four column sections were considered based on practical observations of precast concrete structures commonly used. Two rectangular and two square sections were adopted; the first section being a 40x40 cm^2 column section. These dimensions were chosen with the belief that it is the smallest column size used in precast concrete structures. A normal force was assumed and the corresponding bending moment was calculated following equation 36 for a high eccentricity.

$$\frac{M_d}{N_d \cdot h} \geq 2 \tag{36}$$

From the applied load on the section, the coefficients ν and μ' were calculated according to equations 37 and 38, respectively. Fixing these two coefficients, the internal axial force and bending moment at any other section could be determined.

$$\nu = \frac{N_d}{A_c \cdot f_{cd}} \tag{37}$$

$$\mu' = \frac{M_d}{A_c \cdot h \cdot f_{cd}} \tag{38}$$

Table 4 – Column cross section dimensions and loads

Column section bxh (cm^2)	Axial Force N_d (kN)	Shear Force V_d (kN)	Bending Moment M_d (kN.m)
40x40	250	50	200
40x60	375	112.5	450
60x40	375	75	300
60x60	560	168.75	675

The shear force was determined through a linear ratio with the bending moment, considering the acting of concentrated force. The sections and their respective loads are presented in Table 4. The following material and construction variables were assumed in the design of the rough column:

a) Embedded length for rough interfaces and high eccentricity was based on recommendations by NBR 9062:2006[6]: $\ell_{emb} = 1.6 \cdot h$;

b) Joint width of 5 cm;

c) Pedestal wall thickness: $h_w \geq 1/3.5 \cdot (h_{int}$ or $b_{int})$. This is an intermediary value between the minimum recommended by Campos [5] and that indicated by Leonhardt and Mönnig [15];

d) Steel CA-50 ($f_{yk} = 500$ MPa and $f_{yd} = 435$ MPa) for longitudinal reinforcement and steel CA-60 ($f_{yk} = 600$ MPa and $f_{yd} = 522$ MPa) for transverse reinforcement;

e) Characteristic compression strength of the socket and column concretes: $f_{ck} = 20$ MPa and $f_{ck} = 30$ MPa, respectively, and $\gamma_c = 1,4$.

The formulation proposed in this work assumed a monolithic connection. The obtained results were then compared with the model proposed by Campos et al. [3] adapted for rough interfaces. The geometrical characteristics, internal forces and resulting reinforcements for each section analyzed are presented in Table 5.

Regarding the longitudinal reinforcement A$_s$, the proposed model for rough column base provided values smaller than those obtained from Campos et al. [3] model adapted for rough interfaces. The observed difference is 27% for all cases. Theoretically, no transverse reinforcement would be necessary for the 40x40 cm^2 and 60x40 cm^2 sections based on the proposed model. For the 40x60 cm^2 and 60x60 cm^2 sections, the transverse reinforcements determined according to the proposed model were found to be higher than those obtained from the adapted model for rough interfaces, with the differences up to 28%. The transverse reinforcements obtained from both the proposed model and that adapted for rough interfaces are smaller than the minimum transverse reinforcement recommended by NBR 6118:2007 [17], thus indicating, in this case, the use of minimum reinforcement.

4. Final remarks and conclusions

In this paper, models and design recommendations for the analysis of column-foundation connection through socket with rough

Table 5 – Obtained results for rough interface column base				
Variables	**Column Dimensions (cm^2)**			
	40x40	**40x60**	**60x40**	**60x60**
b_{int} (cm)	50	50	70	70
h_{int} (cm)	50	70	50	70
h_w (cm)	15	20	20	20
b_{ext} (cm)	80	90	110	110
h_{ext} (cm)	80	110	90	110
l_{emb} (cm)	64	96	64	96
l_p (cm)	63	95	63	95
Proposed Model				
β_f	**60°**	**60°**	**60°**	**60°**
β_r	**35°**	**35°**	**35°**	**35°**
R_{csf} (kN)	483.41	815.66	657.41	1222.22
R_{ssf} (kN)	233.41	440.66	282.41	662.22
H_f (kN)	279.10	470.92	379.55	705.65
H_r (kN)	333.34	629.32	403.32	945.75
M_{max} (kN.m)	200.00	450.00	300.00	675.00
N_{max} (kN)	250.00	375.00	375.00	560.00
V_{max} (kN)	104.25	270.90	98.77	408.85
A_s (cm^2)	1099.92	1608.99	1649.89	2416.21
$A_{sw/s}$ (cm)	-	0.272	-	0.417
$A_{swmin/s}$ (cm)	0.444	0.444	0.666	0.666
Campos et al. (3) model adapted for rough interfaces ($\mu= 1$)				
H_{topf} (kN)	312.40	499.43	468.61	749.02
H_{bot} (kN)	162.40	255.68	243.61	384.65
N_{fb} (kN)	100.00	131.25	150.00	195.63
F_1 (kN)	660.00	963.21	990.00	1445.71
F_4 (kN)	162.40	255.68	243.61	384.65
A_s (cm^2)	1518.00	2215.39	2277.00	3325.14
$A_{sw/s}$ (cm)	0.195	0.215	0.292	0.327
$A_{swmin/s}$ (cm)	0.444	0.444	0.666	0.666

interfaces are proposed, contemplating the configuration of the shear keys, the socket and the column base.

After analysis of the theoretical and experimental results, the following conclusions were drawn:

a) For a rough socket foundation to show a behavior similar to that of a monolithic connection, it is necessary that the shear keys dimensions be within the limits recommended in the present work.

b) The design of the vertical reinforcement of rough sockets must be based on the bending theory.

c) The horizontal reinforcement of the transverse walls should be designed following the refined model by Canha et al. [10], adjusting the values of $\beta_f = 60^o$ and $\beta_r = 35^o$ to better represent the experimental results.

d) The new model proposed for analysis of rough column base, calibrated from the socket foundation, was found to present less conservative longitudinal reinforcement compared to the model proposed by Campos et al. [3] and adapted for rough interfaces. The two models were found to provide minimum transverse reinforcement.

It is worth highlighting that the models proposed in this work are valid only for rough interface connections in which the embedded length is determined by the Brazilian Standard Code NBR 9062:2006 [6] and for cases of high eccentricity, keeping in mind that these models were based in experimental observations of specimens within these situations.

5. Acknowledgements

6. References

[01] CANHA, R.M.F.; EL DEBS, M.K. Critical analysis of models and recommendations for designing column-base connection by socket of precast concrete structures. IBRACON Structural Journal, v.2, n.2, p.116-136, June. 2006.

[02] CANHA, R.M.F.; EL DEBS, M.K. Proposal of design model for column-base connection by socket of precast concrete structures. IBRACON Structural Journal, v.2, n.2, p.152-166, June. 2006.

[03] CAMPOS, G.M.; CANHA, R.M.F.; EL DEBS, M.K. Design of precast columns bases embedded in socket foundations with smooth interfaces. IBRACON Structures and Materials Journal, v.4, n.2, p.314-323, June. 2011.

[04] CANHA, R.M.F. Theoretical-experimental analysis of column-foundation connection through socket of precast concrete structures. São Carlos. 279p. PhD Thesis. School of Engineering of São Carlos, University of São Paulo, 2004.

[05] CAMPOS, G.M. Recommendations for the design of socket foundations. São Carlos. 183p. MSc Thesis. School of Engineering of São Carlos, University of São Paulo, 2010.

[06] BRAZILIAN ASSOCIATION OF TECHNICAL STANDARDS. NBR 9062 - Design and fabrication of precast concrete structures. Rio de Janeiro, ABNT. 2006.

[07] RIZKALLA, S.H.; SERRETE, R.L.; HEUVEL, J.S.; ATTIOGBE, E.K. Multiple shear key connections for precast shear wall panels. PCI Journal, v.34, n.2, p.104-120, Mar/Apr. 1989.

[08] LACOMBE, G.; POMMERET, M. Les joints structuraux dans les constructions en grands panneaux prefabriques. Annales de L'Institut Technique du Batiment et dês Travaux Publics, n.314, p.114-144, Fevrier. 1974.

[09] JAGUARIBE JR., K.B. Column-foundation connection through socket of precast concrete structures with reduced embedded length. São Carlos. 167p. MSc Thesis. School of Engineering of São Carlos, University of São Paulo, 2005.

[10] CANHA, R.M.F.; EBELING, E. B.; EL DEBS, A. L. H. C; EL DEBS, M. K. Analysis of the behavior of transverse walls of socket base connections. Engineering Structures, v.31, n.3, p.788-798, Mar. 2009.

[11] NUNES, V.C.P. Experimental analysis of socket foundation emphasizing the internal forces in the pedestal transverse walls. São Carlos. 132p. MSc Thesis. School of Engineering of São Carlos, University of São Paulo,, 2009.

[12] MELLO, C.E.E. (Ed.) MUNTE design handbook of precast concrete. São Paulo: Pini, 2004.

[13] CONSIGLIO NAZIONALE DELLE RICERCHE. CNR-10025 - Istruzioni per il progetto, l´esecuzione ed il controllo delle strutture prefabbricate in calcestruzzo. ITEC/La prefabricazione. Roma, 1998.

[14] EL DEBS, M.K. Precast concrete: bases and applications. 1.ed. São Carlos, SP, Publicação EESC-USP. 2000.

[15] LEONHARDT, F.; MÖNNIG, E. Vorlesungen uber massivbau, Berlin:. Springer-Verlag, 1973. (Portuguese version: Construções de concreto: Princípios básicos sobre armação de estruturas de concreto armado, Rio de Janeiro: Interciência, 1.ed, v.3,. 1977.)

[16] EBELING, E. B. Analysis of precast columns base in the connection with socket foundation. São Carlos. 103p. MSc Thesis. School of Engineering of São Carlos, University of São Paulo, 2006.

[17] BRAZILIAN ASSOCIATION OF TECHNICAL STANDARDS. NBR 6118 - Design of concrete structures - Procedure. Rio de Janeiro, ABNT. 2007.